Check for updates

THE AMERICAN SOCIETY OF MECHANICAL ENGINEERS
Three Park Avenue, New York, N.Y. 10016-5990

99-GT-59

The Society shall not be responsible for statements or opinions advanced in papers or discussion at meetings of the Society or of its Divisions or Sections, or printed in its publications. Discussion is printed only if the paper is published in an ASME Journal. Authorization to photocopy for internal or personal use is granted to libraries and other users registered with the Copyright Clearance Center (CCC) provided $3/article is paid to CCC, 222 Rosewood Dr., Danvers, MA 01923. Requests for special permission or bulk reproduction should be addressed to the ASME Technical Publishing Department.

Copyright © 1999 by ASME All Rights Reserved Printed in U.S.A.

Downloaded from http://asmedigitalcollection.asme.org/GT/proceedings-pdf/GT1999/78590/V002T02A011/4218414/v002t02a011-99-gt-059.pdf by guest on 01 July 2022

COMPARISON BETWEEN MEASURED AND PREDICTED WALL TEMPERATURES IN A GAS TURBINE COMBUSTOR.

BREAK

R.A. Hicks* and C.W. Wilson
Propulsion Department, , Defence and Evaluation Research Agency,
Farnborough, United Kingdom, GU14 0LS

ABSTRACT

On of the major considerations in the development of advanced gas turbine engines are increased thrust to weight ratio and reduced development and operating costs. Improvements in engine thrust require an increase in combustion chamber heat release and inlet pressures. However, increasing the amount of heat release will also result in an increase in the radiative heat flux to the combustion chamber walls, proving detrimental to the operational life time of the combustor. To maximise combustor life, different cooling devices can be incorporated into the combustion chamber design. The effectiveness with which these devices are implemented is important and in the absence of a reliable predictive numerical tools, is difficult to quantify without undertaking expensive and timely testing. A computer analysis tool, based on a network model approach, has previously been developed to analyse airflow distributions in complex combustor geometries. A recent variant of this model has incorporated the Discrete Transfer radiation model, along with other convective and conductive sub-models, to account for heat transfer. These models have heen validated against thermocouple measurements of wall temperature obtained in a sectored research combustor. The results of this comparison indicate that, whilst the model is capable of predicting the trends in wall temperature, it is currently unable to reproduce the magnitude of wall temperature with a greater accuracy than 80 K. However, the versatility of the discrete transfer model suggests that further improvements in accuracy are possible.

INTRODUCTION

One of the major considerations in the development of advanced gas turbine engines are increased thrust to weight ratio and reduced development and operating costs. Improvements in engine thrust require an increase in combustion chamber heat release and inlet pressures. Increased heat release can be achieved by operating the combustor at a richer overall air fuel ratio (AFR) combined with improved combustor primary zone mixing. However, increasing the amount of heat release will also result in an increase in the total radiative heat flux to the combustion chamber walls, one of the principle components of heat transfer in a gas turbine combustor [1, 2]. Such an increase in heat flux could prove detrimental to the operational life time of the combustor.

To maximise combustor life, a number of different cooling devices can be incorporated into the combustion chamber design, either separately or in combination. With the exception of ceramic thermal barrier coatings, these devices utilise some

* Corresponding author.

© British Crown copyright 1999. Published with the permission of the Defence Evaluation & Research Agency on behalf of the Controller of HMSO

Presented at the International Gas Turbine & Aeroengine Congress & Exhibition
Indianapolis, Indiana — June 7–June 10, 1999

of the combustion chamber/annuli air flow, either directly, as in the case of film cooling techniques such as 'Z' ring and effusion patch cooling methods, or indirectly, by incorporating ribs onto the outside wall of the combustion chamber. The effectiveness with which these cooling devices are implemented in a combustion chamber design is important from two points of view. First of all is their ability to maintain the combustor walls at an acceptable temperature. However, an equally important consideration is how much of the inlet air flow is required to achieve this. The injection of large amounts of cooling air can have an adverse effect on emission control and thus, should be minimised. In the absence of a reliable predictive numerical tool however, it is difficult to quantify the effectiveness of a combustor's cooling strategy without undertaking expensive and timely testing.

Network methods [3] have demonstrated their ability to predict flow distributions for complicated and unusual combustor geometries effectively, whilst retaining the advantage of rapid execution. The network method relies on a system in which an arbitrary geometry is divided into a number of independent sub-flows linked together to model a physical process. Recent incarnations of this approach [4] have included heat transfer analysis. Experimental thermal paint data was used to validate the heat transfer model [5]. However, this proved to be inadequate as the bandwidth of the thermal paint data were too wide to accurately compare with computed combustor wall temperatures. Therefore, a programme of work has been undertaken to generate more precise experimental data on combustor wall temperatures. This paper describes the experimental work and discusses the validity of the corresponding network model (FLOWNET) predictions, and models therein.

EXPERIMENTAL MEASUREMENTS

Wall temperature measurements were obtained using a four burner annular combustor sector for which experimental thermal paint data was available from an earlier test programme; although only available for one set of operating conditions, the availability of thermal paint data would allow some confirmation of measured wall temperatures. The design of the combustor incorporated both 'Z'-ring and angled effusion film cooling devices, Figure 1. External heat transfer to the inner and outer annuli air flows was enhanced through the use of ribs. In addition to these aerodynamic cooling devices, the inside, 'hot' surface of the combustor was coated with a thermal barrier coating (TBC). The coating, which was of the order of 0.5 mm thick, was applied from half way along the first Z-ring cooling 'bay' (Figure 1) to the rear of the combustor.

To provide an accurate measurement of combustor wall temperatures, the research combustor was fitted with twenty four 'K' type (Chromel/Alumel) thermocouples. The thermocouples were attached to the outer wall of the combustor only and distributed evenly down the length of the combustor, as indicated in Figure 2. Circumferentially, the thermocouples were fitted equi-spaced between one of the primary ports and the approximate mid-way point to the adjacent primary port, Figure 2. To ensure that only the inner wall temperature was recorded, the 'hot' junction of each thermocouple was located in a small recess in the combustor wall and held in place using a high temperature ceramic adhesive, as illustrated in Figure 3. This approach has previously been used to successfully measure gas turbine combustor wall temperatures [6].

The fragile nature of the thermocouple hot junction, which were made from 0.13 mm diameter wires, meant that each thermocouple had to be housed in a 1 mm diameter, 1 meter long protective stainless steel sheath. The tip of the sheath, into which the hot junction of the thermocouple was embedded, was then swaged down to 0.5 mm diameter to ensure that, when attached to the combustor, the thermocouple accurately recorded the wall temperature.

The instrumented combustor was mounted on the Sector Combustion Rig (SCR) test facility located at DERA. The outputs from the twenty four thermocouples were recorded simultaneously using a Datascan multichannel data logging system, used inconjunction with MTX Pro-pack data logging software, at a rate of 0.1 Hz. To ensure that the thermocouples were working correctly, they were calibrated agianst the measured inlet air temperature, which was varied over a several different values, with the combustor operated 'cold', i.e. no combustion; in the absence of combustion, the combustor wall temperature corresponds to the inlet air temperature.

A reference test condition, based on the maximum rig capability, was defined that matched the experimental test condition at which the thermal paint data had previously been obtained; inlet pressure of 9 bar, inlet temperature equal to 820 K and a combustor air/fuel ratio of 29:1. In addition to this reference condition, data were also obtained for a number of other inlet conditions, as listed in Table 1. Typically, thirty samples were taken at each condition and then averaged to find the mean wall temperature distribution along the length of the combustor. By considering a range of different sample times and numbers, mean wall temperatures derived from 30 samples were found to be stationary. The variance in measured temperature values, along with the corresponding mean, maximum and minimum temperature values are tabulated in Table 2. To ensure that no transient effects were present in the measured data, the combustor was allowed to achieve steady state operation before measurements were performed. Steady state operation was typically achieved after about 5 minutes running on station.

Downloaded from http://asmedigitalcollection.asme.org/GT/proceedings-pdf/GT1999/78590/V002T02A011/4218414/v002t02a011-99-gt-059.pdf by guest on 01 July 2022

THE FLOWNET COMPUTER CODE

FLOWNET is a one dimensional computer simulation model which solves complex flow network problems. The original program was produced by 'M-TECH mechanical'; a company based in South Africa and is a commercially available computer code. However, the basic FLOWNET model has been adapted for combustor analysis by Cranfield University [3]. This has involved the inclusion of a number semi-empirical sub-models to represent various features pertinent to a gas turbine combustor. Features considered include such things as cooling/dilution ports, diffusers, pedestals and pin-fins. A gas properties package has also been incorporated in the model to allow the products of combustion to be computed for various efficiency levels [5].

For a gas turbine combustor, FLOWNET divides the combustor into a series of one-dimensional sub-flows (bits), containing independent semi-empirical governing equations, depending upon the feature modelled. Each individual feature of the combustor, such as cooling holes, injectors, etc. can be represented by combinations of bits & elements. These are then linked together by the overall governing equations, to obtain a complete solution of the entire flow field.

The global flow splits and pressure-drops are obtained throughout the combustor using a pressure-correction methodology, which ensures mass continuity. The solution for the energy equation is obtained using a Gauss Seidel scheme [5].

The heat transfer analysis incorporated into FLOWNET accounts for conduction, convection and radiation within the region of the combustor [5]. The convection models include the effect of combustor film cooling. Film cooling flows introduced at different axial locations along the combustor may accumulate. Therefore, to account for this, FLOWNET allows a maximum of three films to overlap in this way. Radial and/or axial conduction through multi-layered walls (i.e. thermal barrier coating/metal wall combinations) are also included within the analysis.

Initially, the only radiation model available in the heat transfer analysis made use of a simple semi-empirical relationship [5]. This model, which is based on a luminosity factor [10] and the approach outlined in Lefebvre [2], has only proved capable of providing qualitative agreement with experimental results [5]. This was thought to be associated with the gross simplification made in using bulk gas emissivities, derived from empirical data obtained at pressure below 500 kPa and fuel/air ratios weaker than stoichiometric, bulk pressure, bulk temperature, mean beam length and a soot luminosity factor, all of which made no account of radial or circumferential variation of the properties. Consequently, the heat transfer model incorporated into FLOWNET was extended to include the Discrete Transfer radiation model [7].

The Discrete Transfer method, the implementation of which into FLOWNET is described fully in Reference 4, involves tracing representative 'rays' from one combustor surface to another through the region of interest. For each ray, an intensity distribution is calculated along its length, as a function of a user defined temperature and soot loading distribution, as it passes through the domain. The intensities of the individual rays are then summed at the various wall locations to give the net radiative heat flux.

RESULTS AND DISCUSSION

Shown in Figure 4 is the network representation of the research combustor used in this study. The individual bits define the various features of the combustor, such as primary and dilution ports, cooling features, inlet diffuser duct, etc.. These bits are inter-connected with each other via nodes (not shown in the figure for clarity purposes). Each bit/node combination represents a computational cell in which the flow and energy equations are solved. The heat transfer model components are represented by the bits FHT, CD and AHT, corresponding to 'flame tube heat transfer', 'wall conduction' and 'annulus heat transfer', respectively.

For the work reported here, an existing air flow network model for the combustor was modified to include heat transfer sub-models. The inclusion of the heat transfer sub-models into the network allowed for the effects of mixing, film cooling, radiation and conjugate heat transfer through the double skin (i.e. TBC/wall) regions of flametube walls to be considered. Initially, this 'heat transfer' network was laid out by simply adding heat transfer elements between the relevant flametube/annulus bits in the existing air flow network. This meant that the network was set up in such a way that corresponding numbers of bits appeared in both the flametube and the annulus, thus allowing uniformity in computed surface area of heat transfer between the two regions. However, with this network configuration, it proved impossible to obtain a converged solution. To overcome this problem, it was necessary to modify the network by moving the point at which the film cooling air flows were added into the flametube bits downstream of their original location, which was perpendicular to the adjacent flametube bit. This made the network more representative of the actual physical flow addition situtation within the combustor and as a result, change the ratio between the predicted combustor and the cooling film gas velocities. This ratio is important as it controls the effective cooling length of the film [8]. Consequently, it is an important parameter in the formulation used to model Z-ring convective film cooling.

When considering the inclusion of the heat transfer model, two issues arose with regards to defining the layout of the network. The first of these was the influence on predicted wall temperatures of the cooling film carry over from one feature to the next. The combustor incorporated effusion patch cooling at

Downloaded from http://asmedigitalcollection.asme.org/GT/proceedings-pdf/GT1999/78590/V002T02A011/4218414/v002t02a011-99-gt-059.pdf by guest on 01 July 2022

the head of the combustor (Figure 1), augmented by cooling films being fed from air flows exiting the baseplate/heatshield assembly. This initial film cooling is continued downstream by the inclusion of additional Z-rings, as illustrated in Figure 1.

The role of cooling film devices is to generate a protective film of cooling air between the wall and hot combustion gases. This cooling film however is gradually destroyed by turbulent mixing with the hot gas stream and as a result, has a finite length of effectiveness [2, 8]. This may, or may not, include extension of the cooling film into the next cooling bay. For this combustor, no data was available to indicate whether or not cooling film carry over occurred. However, included in the Z-ring cooling correlation in the heat transfer model is an option to consider the continuation of one cooling film into another. To assess the influence such continuation might have on estimated wall temperatures, the heat transfer model was executed with and without this option.

Shown in Figure 5 are predicted wall temperatures with and without cooling film carry over. Although there is some scatter in the data (due to the number of elements used to model the combustor), it is arguable that the inclusion of film cooling carry over has lead to a reduction in the predicted wall temperature. For this combustor, the baseplate/effusion film cooling flow is sufficently large [9] to suggest that carry over may occur [9] and as a result, for the work reported here, the model was operated with cooling film carry over.

The second point of uncertainty was the influence of port flows on predicted wall temperatures. The cooling film in the vicinity of the port will be destroyed by the jetting action of the port flow. However, it is arguable that, if the inter-port spacing is sufficiently large, the cooling film will remain unperturbed by the port flow, thus providing some cooling. At present the correlations incorporated within the heat transfer model have no way to account for this and its influence could therefore not be assessed.

Shown in Figure 6 are mean thermocouple temperature data for the inner 'hot' surface of the outer flametube wall with the combustor operating at a rig limited reference inlet condition of 9 bar, 820 K combustor air/fuel ratio of 29:1. Also plotted on this figure are the corresponding FLOWNET predicted wall temperatures for this condition. These predictions were obtained using the Discrete Transfer radiation model. FLOWNET is unable to discriminate temperature gradients in the circumferential direction. Consequently, for comparison purposes, the experimental data were averaged in the circumferential direction (Figure 2). Indicated by the hatched areas in Figure 6 are the bandwidths corresponding to thermal paint temperature data obtained using a nominally identical combustor geometry. These data, obtained as part of an separate programme, were taken from the painted 4 burner sector pictured in Figure 2.

The first row of thermocouples (at an axial distance, relative to the front of the combustor, of 0.04 m) have recorded the highest mean wall temperature at about 950 K. At this location, no thermal barrier coating is present and cooling is purely by film cooling. At the other measurement locations downstream of this point, the thermocouples indicate that the wall temperature is fairly uniform at a mean temperature of about 820 K. At the rear of the combustor, the thermocouple measurements increase slightly. This is believed to an artifact of the thermocouple measurement rather than any real increase in temperature. With the exception of the middle of the combustor, the thermocouple measurments show similar temperatures to those recorded by the thermal paint data (hatch area on Figure 6). The reason for the discrepancy in the middle of the combustor is probably associated with a localised hot spot on the thermally painted combustor which was not thought to be present on the instrumented combustor.

To allow accurate assessment of combustor life performance, FLOWNET must be able to predict the combustor wall temperature to within an accuracy of 5 K. Comparison between the FLOWNET predicted wall temperatures and the corresponding thermocouple data in Figure 6 shows that, although the general trend has been reproduced, the network solver has over predicted the wall temperature by approximately 80 K relative to thermocouple measurements; although this discrepancy drops to about 40 K at the front of the combustor. Clearly, the target accuracy is not being met by FLOWNET. However, given the complexity of gas turbine combustion, a worst case discrepancy of about 80 K between prediction and measurement is encouraging.

One reason for the difference between the sets of data could be the accuracy of the calculated hot gas temperature in the flametube. Shown in Figure 7 is the one dimensional hot gas temperature calculated by the network solver for the reference inlet condition; 815 K at 915 bar and 29:1 combustor AFR. The calculation procedure included the use of a constrained equilibrium model, constrained for CO and CO_2. Efficiency curves for an annular airspray combustor were used in computing these constraints. A mixing model [3] was used to compute the fuel/air ratio used in the equilibrium model.

Also plotted on Figure 7 are mean one dimensional experimental values of gas temperature at three different axial locations within the combustor. The agreement between the measurement derived and predicted temperature values at all planes is good.

The mean empirical data plotted in Figure 7 were derived from measured two dimensional profiles of gas temperature obtained as part of a separate research programme; the location of the measurement planes are indicated on Figure 1. The empirical temperature data were calculated from species measurements made within the combustor using an internal traversing sample probe. The stainless steel probe, incorporating high pressure

Downloaded from http://asmedigitalcollection.asme.org/GT/proceedings-pdf/GT1999/78590/V002T02A011/4218414/v002t02a011-99-gt-059.pdf by guest on 01 July 2022

water cooling, had four axes of freedom within the combustor: left/right, horizontal/vertical, in/out and rotational. In addition to these degrees of freedom, the probe shape was interchangable to allow the complete inner space of the combustor to be accessed. Species measured included carbon dioxide (CO_2), carbon monoxide (CO), oxygen (O_2), unburnt hydrocarbons (UHC), oxides of nitrogen (NOx), nitric oxide (NO) and hydrogen (H_2). Smoke measurements were also been made using two techniques: SAE filter paper and an optical method, the Sigrist smoke meter. To prevent condensation, the samples from the sample probe were transferred to the gas anlaysis system through a heated line, maintained at a temperature of 150 °C, ± 5°C. From these data, along with readings for ambient pressure and temperature and dew point, estimates of water (H_2O), nitrogen (N_2) and nitrogen dioxide (NO_2) concentrations, and local AFR and gas temperature were made.

The Discrete Transfer method incorporated within FLOWNET allows for the use of different user defined soot volumes fractions in both the radial and axial directions. These provide a measure of the flame's 'optical' density. If sufficiently dense, a flame will only radiate heat from it's surface. In contrast, a flame of lower optical density will radiate heat not only from it's surface but also from within the flame brush.

The magnitude and profile of soot volume fractions used in the DT radiation model in the work reported here were derived from soot fraction measurements also obtained from within the sectored combustor using the internal traversing probe discussed earlier. As a result, the magnitude of the soot volume fractions that could be used for modelling the reference inlet condition were fixed by the available experimental data. However, whilst the magnitude of soot volume fraction was fixed, it was possible to vary the radial soot volume profile, to which the wall temperatures predicted by FLOWNET were found to be very sensitive. Shown in Figure 8 are wall temperatures calculated using two different radial soot profiles, as illustrated in Figure 10; the corresponding heat fluxes are given in Figure 9. Although it could be argued that the one dimensional soot profile gives a good representation of an average soot volume fraction, the two dimensional profile shown in Figure 10, with a decay in soot concentration at the combustor walls, is more representative of the actual soot profile, if still coarse when compare to the measured data, Figure 11.

The soot loading profile shown in Figure 11 is typical for the combustor at an axial location just downstream of the dilution ports (Plane D in Figure 1). As can be seen the soot profile should ideally be supplied as a three dimensional profile. In an effort to account for this, an attempt was made to apply a more sophisticated 2D radial profile to the model. Unfortunately, such a profile resulted in a failure of the model. This reason for this failure is currently unclear and is receiving further attention.

As a result of the introduction of a two dimensional soot profile, the predicted wall temperature was found to fall by about 150 K. Such sensitivity to a relatively minor change in radial soot profile would suggest that, for the reference inlet condition, the flame is optically thick and that the heat flux is the result of flame surface radiation. However, a drawback of the sensitivity of predicted wall temperature to the soot loading profile would indicate that, as an predictive tool, the heat transfer model would require a reasonable knowledge of the soot distribution in the combustor. Such information may only be available as a result of a experimental test programme.

However, although the inclusion of the two dimensional soot profile has improved the prediction, FLOWNET still over predicts the measured data by a significant amount. A possible reason for this is that, although the two dimensional soot profile reproduces the global features of the measured soot loading profile (as illustrated Figure 11), it does not replicate the local radial and circumferential variations in soot concentration. Given the sensitivity shown by the model to soot loading, such variations may be important. As noted earlier, an attempt has been made to adopted a more sophisticated soot profile but this caused the model to fail. At present, this is currently undergoing investigation. A further source of error are the use of global combustor gas and pressure profiles, with no account taken of radial or circumferential variations. Both of these parameters will impact on the predicted radiative heat flux.

Shown in Figures 8 and 9 are the calculated wall temperatures and heat flux obtained with the semi-empirical radiation model. With this model, the resulting wall temperatures and heat flux are similar to those obtained with the one dimensional soot profile in the DT radiation model; this is a similar finding to that of earlier work undertaken at Cranfield University in a separate programme of work on a different combustor [5]. However, perhaps this is not surprising that the semi-empirical model greatly over-predicts the wall temperature given the simplifications associated with this method, as discussed earlier. Nevertheless, the results shown in Figures 8 and 9 indicate the the current semi-empirical correlation approach is inadequate when trying to achieve reliable predictions of wall temperature and that a more sophisticated approach, such as the DT method, is required.

The variation in measured and predicted wall temperatures with combustor AFR at a inlet pressure and temperature of 7 bar and 850 K, respectively, is presented in Figure 13. In obtaining these data, the DT radiation model was used in conjunction with the 2D soot volume fraction profile. For the 26:1 AFR case, the soot volume fraction was considered to be the same as that at the reference inlet condition. However, to allow for the fact that the magnitude of soot would fall with increasing AFR,

Downloaded from http://asmedigitalcollection.asme.org/GT/proceedings-pdf/GT1999/78590/V002T02A011/4218414/v002t02a011-99-gt-059.pdf by guest on 01 July 2022

the soot volume fraction for the other two cases in Figure 13 was assumed to reduce linearly with increases in AFR.

At the axial location of 0.04 m, it is noticeable that as the combustor AFR is increased, the measured wall temperature falls. This is associated with a corresponding fall in gas temperature within the combustor, as indicated in Figure 14. At a combustor AFR of 26:1, the network solver predicts a maximum gas temperature of about 2300 K downstream of the primary ports. This is because at this location the local AFR is near stoichiometric. As dilution air is introduced further downstream, the gas temperature can be seen to fall. However, the introduction of larger AFR's changes both the value of the peak temperature, which reduces, and the location at which it occurs. The shift in peak temperature towards the fuel injector is due to the fact that, under very lean conditions, the rich region immediately downstream of the fuel injector is the only location at which the stable combustion can be achieved.

With regards to the other thermocouple locations in Figure 13, a change in gas temperature with AFR is not registered. Here, the thermocouples record a wall temperature that is fairly uniform at about 850 K. This is the same as the inlet air temperature used for these experiments, suggesting that the thermal barrier coating is working effectively as a thermal block. However, it is interesting to note that, because the metal wall liner temperature (as indicated by the thermocouples) remains constant, the temperature gradient across the TBC must be varying as the gas temperature within the flametube varies. This thermal stress may prove detrimental with regards to the life span of the TBC.

Unlike the thermocouple measurements, the predicted wall temperatures do not indicate a fall in temperature in the primary zone region of the combustor as the AFR is increased. In general, the FLOWNET predictions suggest that there is little change in wall temperature as the mixture strength is reduced. As noted earlier with regards to Figure 6, the predicted wall temperatures are again larger than those recorded by the thermocouples.

The variation in measured wall temperature with inlet temperature at two different inlet pressures are shown in Figures 15 and 16. As the inlet temperature is increased at both pressures, the thermocouple data increases by a similar amount. This again indicates that the thermal harrier coating is working well and that the temperature of the liner is principally governed by the inlet air temperature in the TBC region. As noted in the discussion of Figure 13, the measured wall temperature in the region of no TBC at the front of the combustor (0.04 m axial location) show the highest value at all three inlet temperatures. And as with the other experimental data presented in these figures, the change in wall temperature follows the change in inlet temperature.For both inlet pressures, the network solver has reproduced the sensitivity of the wall temperature to inlet temperature indicated by the thermocouple measurements. However, as with the other predicted wall temperatures presented in this report, the model is over predicting the wall temperature by varying degrees of accuarcy. In general, the degree of over prediction remains constant, suggesting that the model is reproducing the salient features of the combustion process.

CONCLUSIONS

Predictions of combustor 'hot' wall temperatures have been compared with thermocouple wall temperature measurements undertaken in a 4 burner sector research combustor for a range of operating conditions. The predictions have been obtained using a one-dimensional model based on the network approach. The model, FLOWNET, incorporated the Discrete Transfer radiation model, as well as sub-models for convection and conduction wall heat transfer and other flow features of the combustor.

Measured thermocouple wall temperatures compared well with thermal paint data at an inlet condition of 9 bar, 820 K and and combustor AFR of 29:1. The similarity of the thermocouple data and the thermal paint data with the inlet air temperature suggests that in regions where a thermal barrier coating is applied to the combustor, the combustor wall is effectively protected against radiative/convective heat flux.

Comparison between the measured wall temperature data and those predicted by the network model indicated that, for all the experimental conditions considered, the model is capable of reproducing the trends indicated by the thermocouple data. However, the network solver consistently over-predicted the magnitude of the wall temperature by 80 K. The value of the wall temperature was found to be very sensitive to the radial profile of soot volume fraction supplied to the discrete transfer model by the user. The best predictions of wall temperature were obtained using a 2D radial soot profile in which the soot volume fraction was allow to fall to zero in the vicinity of the wall. This profile was representative of experimentally measured soot volume fractions for the combustor being considered. However, futher improvements in the value of the predicted wall temperature may be possible if more precise radial and circumferential variations in soot, gas temperature and gas pressure are adopted.

Comparison between predictions made using the Discrete Transfer radiation model and a more simplistic semi-empirical radiation model, indicated that the semi-empirical approach was inadequate if reliable predictions of wall temperature are required.

ACKNOWLEDGEMENTS

The authors would like to acknowledge Rolls-Royce Plc, and in particular Mr Mark Jefferies, for use of the FLOWNET network model and experimental data and Dr Phil Rubini of Cranfield University for helpful discussions on this work.

Downloaded from http://asmedigitalcollection.asme.org/GT/proceedings-pdf/GT1999/78590/V002T02A011/4218414/v002t02a011-99-gt-059.pdf by guest on 01 July 2022

REFERENCES

1. Eklund, D.R., Badinand, T and Fransson, T., *A Numerical study of Radiation Effects in Gas Turbine Combustion Chambers.*, AIAA technical paper 98-3822, 1998.
2. Lefebvre, A.H., *Gas Turbine Combustion*, McGraw-Hill Book Company USA, 1983
3. Stuttaford, P.J. and Rubini, P.A., *Preliminary gas turbine combustor design using a network approach.*, ASME technical paper no. 96-GT-135, 1996.
4. Stuttaford, P.J. and Rubini, P.A., *Assessment of a Radiative Heat Transfer Model for a New Gas Turbgine Combustor Preliminary Design Tool.*, 38th AIAA Conf., Reno, Nevada, Jan. 1997.
5. Stuttaford, P.J., *Preliminary Gas Turbine Combustor Design Using a Network Approach.*, PhD. Thesis, Cranfield University, England, 1997
6. Stetson, K.A., *Demonstration Test of Burner Liner Strain Measuring System.*, NASA Report R84-926376-15, June 1984.
7. Lockwood, F.C. and Shah, N.G., *A New Radiation Solution Method for Incorporation in General Combustion Prediction Procedures*, Proceedings of the Eighteenth Symp. (Int.) on Combustion, The Combustion Institute, Pittsburg, pp. 1405-1414, 1984
8. Stollery, J. L. and El-Ehwany, A. A. M., *A Note on the Use of a Boundary-Layer Model for Correlating Film-Cooling Data.*, Int. J. Heat Mass Transfer, 8, no. 1, pp. 55-65, 1965.
9. Jefferies, M.J., Rolls-Royce plc., *Private communication*, January 1998.
10. Mellor, A.M., (ed.), *Design of Modern Turbine Combustors.*, Academic Press Ltd., London, 1990

Condition	P_3 (bar)	T_3 (K)	AFR_{CC}
ref.	9	820	29:1
1	5	750	26:1
2	5	800	26:1
3	5	850	26:1
4	7	750	26:1
5	7	800	26 :1
6	7	850	26:1
7	9	750	26:1
8	9	800	26:1
9	9	850	26:1
10	7	850	26:1
11	7	850	43.8:1
12	7	850	53.2:1

Table 1. Combustor inlet test conditions.

Cond.	Front of Combustor			
	T_{mean}	T_{max}	T_{min}	$\%_{var}$
ref.	942	971	907	6.8
1	878	921	850	8.1
2	876	916	841	8.5
3	887	930	847	9.3
4	928	949	895	5.8
5	942	970	904	7
6	940	984	903	8.6
7	971	995	944	5.2
8	984	1007	951	5.7
9	993	1021	956	6.5
10	984	1007	951	5.7
11	946	966	925	4.3
12	912	927	840	9.5

Table 2. Variance in temperature measurements for front of combustor

Cond.	TBC region			
	T_{mean}	T_{max}	T_{min}	$\%_{var}$
ref.	824	834	805	3.5
1	788	830	744	10.9
2	779	823	744	10.1
3	786	840	750	11.5
4	806	856	793	7.8
5	811	873	794	9.7
6	825	878	794	10.2
7	853	903	840	7.4
8	857	916	841	8.8
9	861	875	848	3.1
10	857	916	841	7.8
11	851	893	839	6.3
12	847	873	828	5.3

Table 3. Variance in temperature measurements for TBC region of combustor.

Downloaded from http://asmedigitalcollection.asme.org/GT/proceedings-pdf/GT1999/78590/V002T02A011/4218414/v002t02a011-99-gt-059.pdf by guest on 01 July 2022

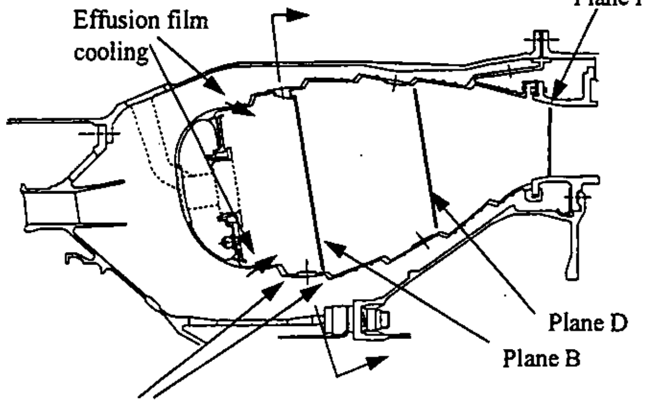

Figure 1; Cross section of combustor assembly. Planes on figure indicate locations at which temperature and soot data were available.

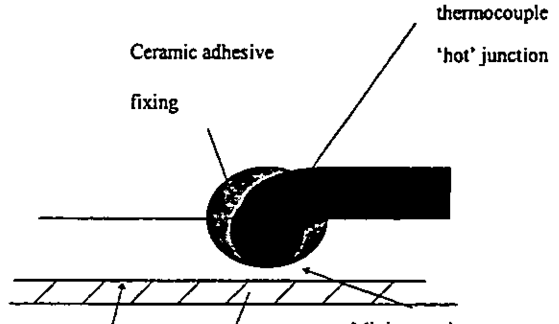

Figure 3; Pictorial representation of technique used to attached thermocouple to combustor wall.

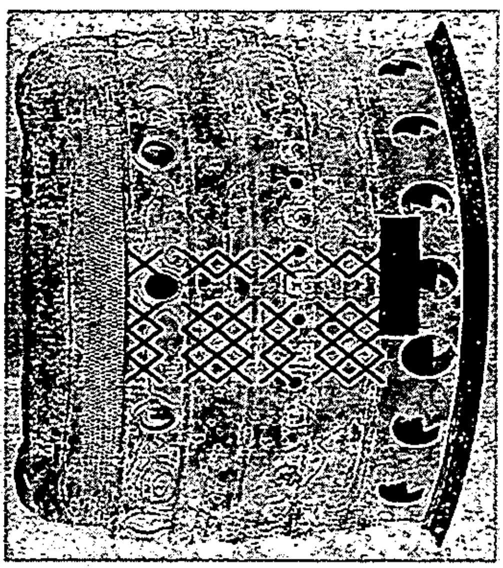

Figure 2; Plan view of sectored research combustor. Crosses indicate location of thermocouples on outer combustor wall.

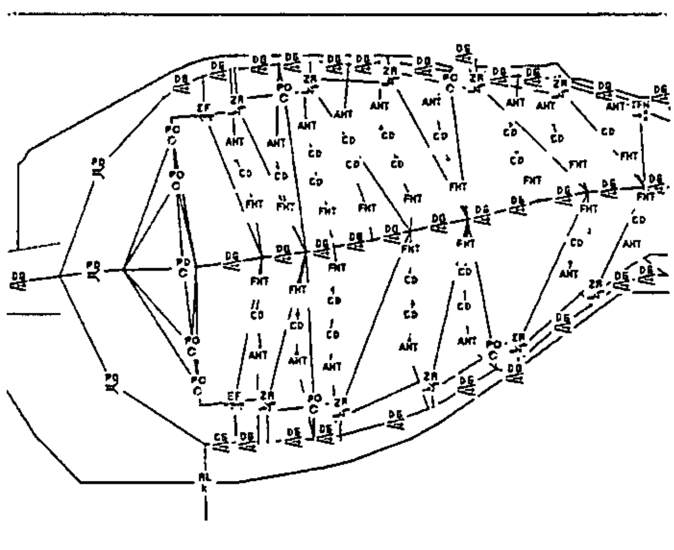

Figure 4; Combustor FLOWNET network representation.

Downloaded from http://asmedigitalcollection.asme.org/GT/proceedings-pdf/GT1999/78590/V002T02A011/4218414/v002t02a011-99-gt-059.pdf by guest on 01 July 2022

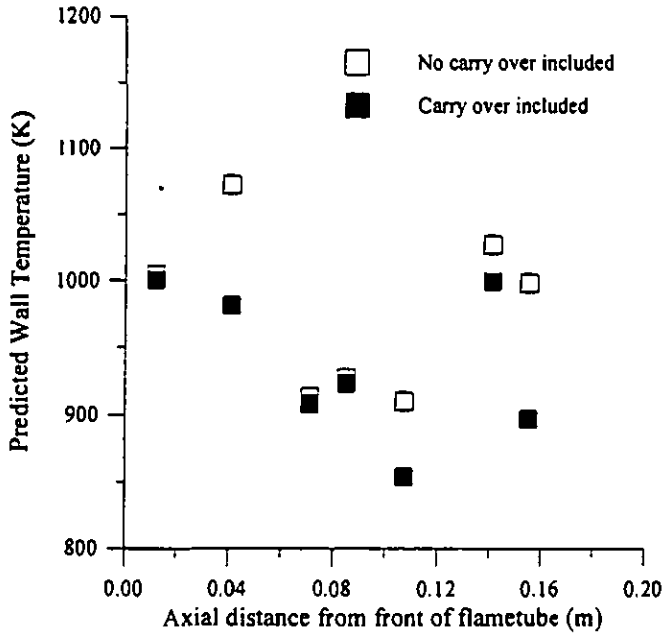

Figure 5; Influence of carried over cooling films on predicted wall temperature.

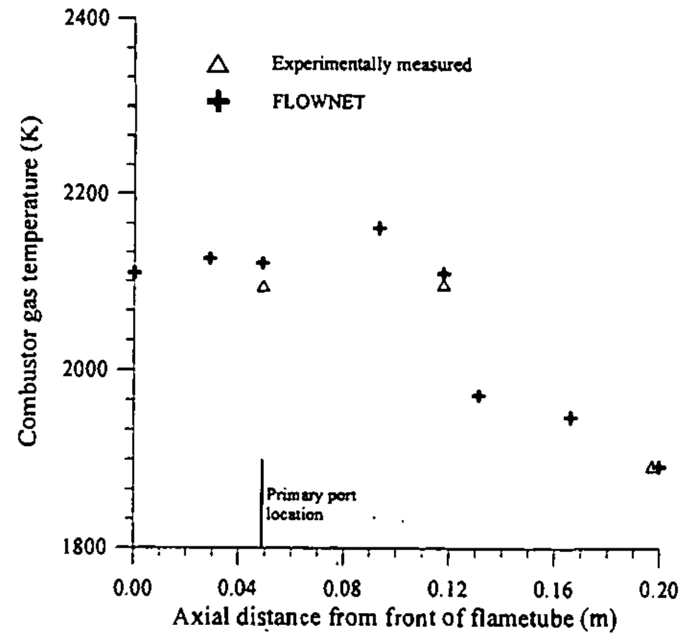

Figure 7; FLOWNET predicted flametube gas temperature compared with experimental values.

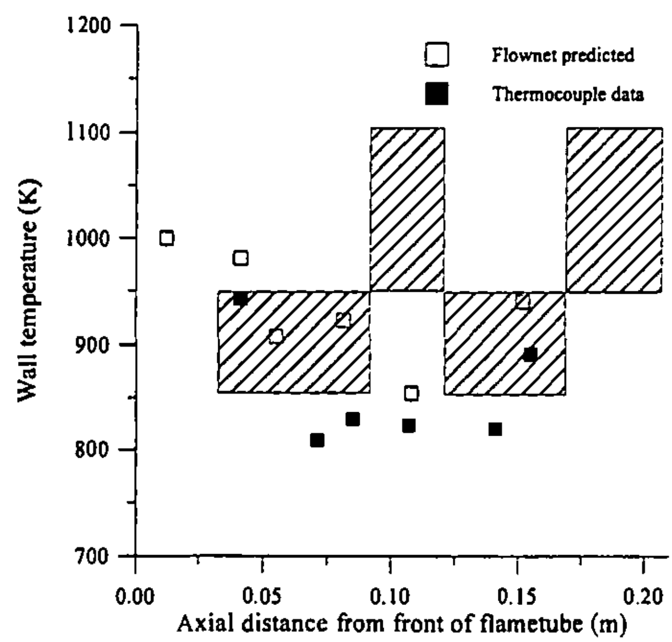

Figure 6; Comparison between predicted and measured wall temperatures. Hatch area indicates thermal paint band widths.

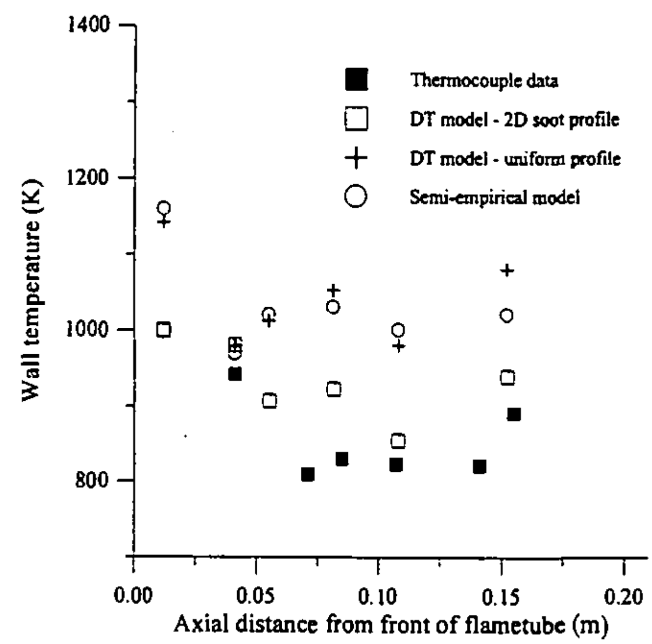

Figure 8; Influence of radiation model on predicted wall temperatures.

Downloaded from http://asmedigitalcollection.asme.org/GT/proceedings-pdf/GT1999/78590/V002T02A011/4218414/v002t02a011-99-gt-059.pdf by guest on 01 July 2022

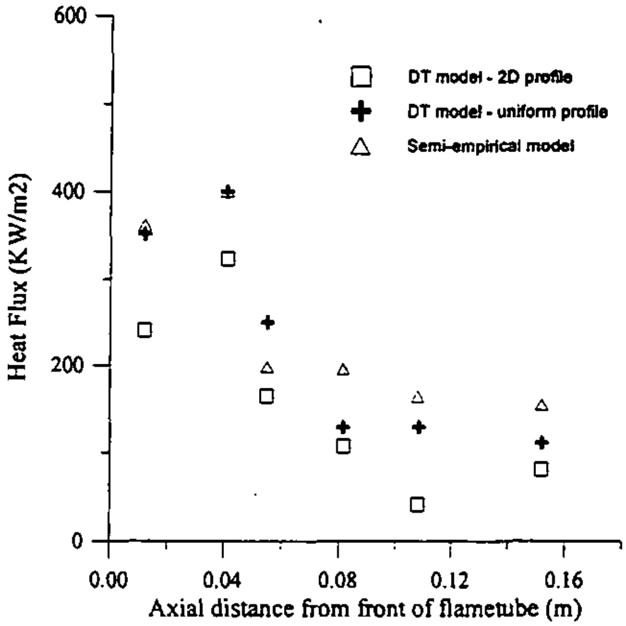

Figure 9; Influence of radiation model on predicted heat flux to wall.

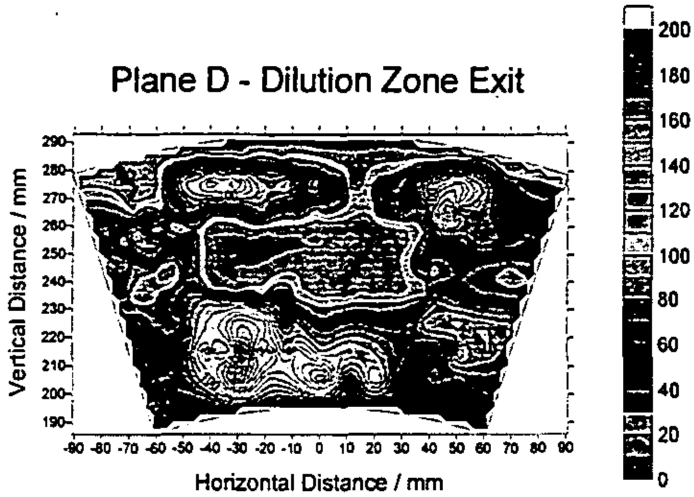

Figure 11; Soot loading profile for research combustor (units: mg/m^3).

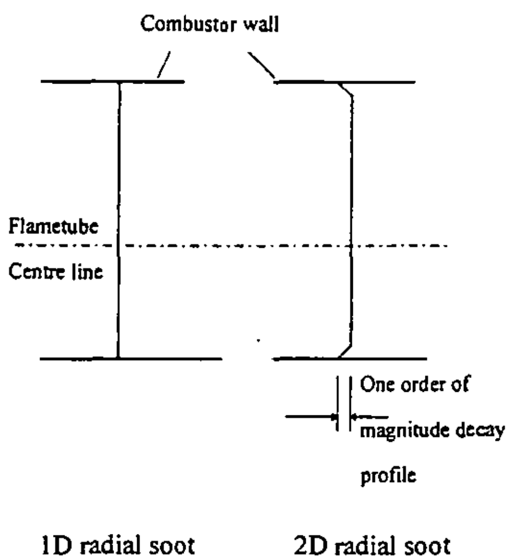

Figure 10; Radial soot profiles used in DT radiation model.

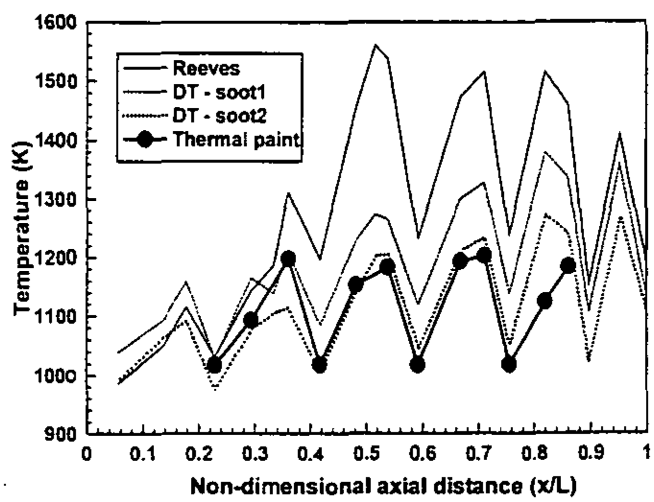

Figure 12; Cranfield University comparison between soot radiation models.

Downloaded from http://asmedigitalcollection.asme.org/GT/proceedings-pdf/GT1999/78590/V002T02A011/4218414/v002t02a011-99-gt-059.pdf by guest on 01 July 2022

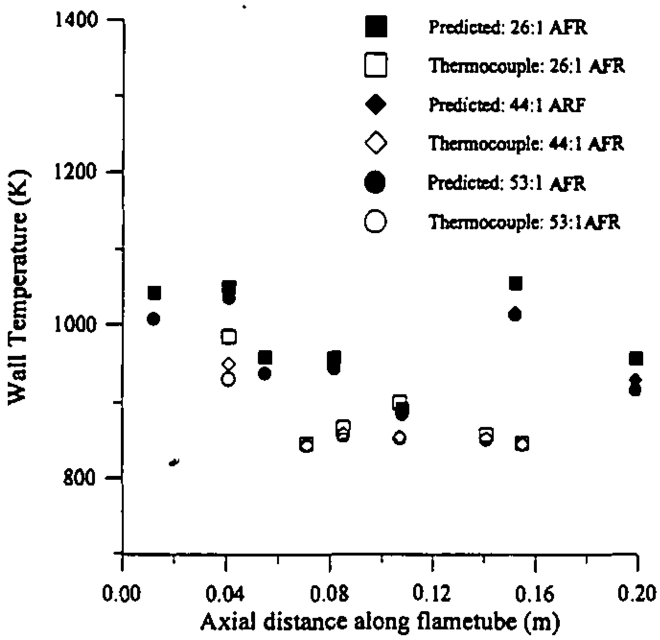

Figure 13; Change in measured and predicted wall temperature with combustor AFR.

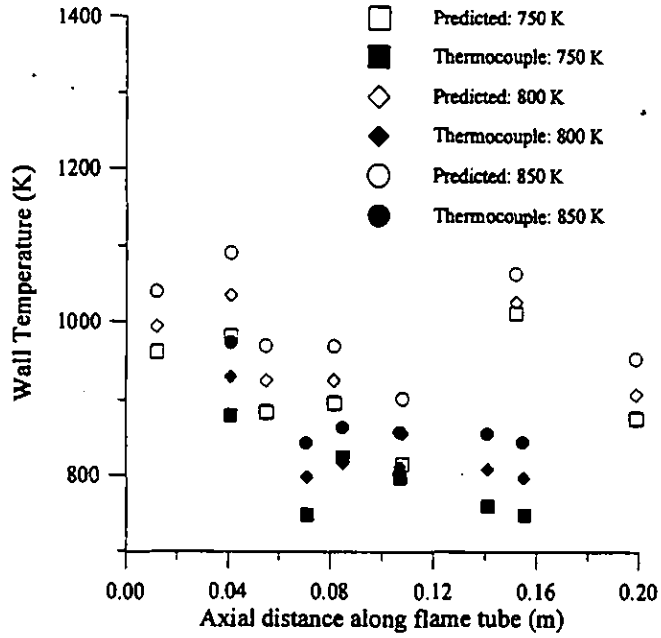

Figure 15; Influence of temperature on wall temperature at an inlet pressure of 5 bar.

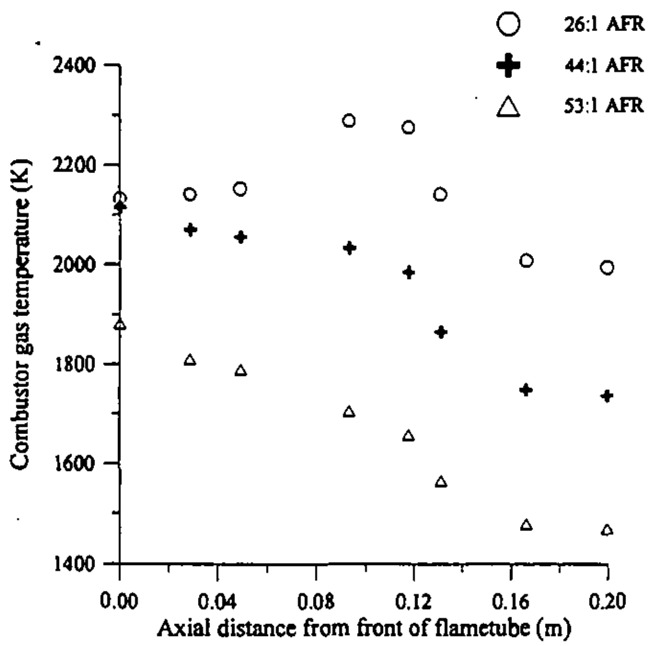

Figure 14; Change in gas temperature with combustor AFR.

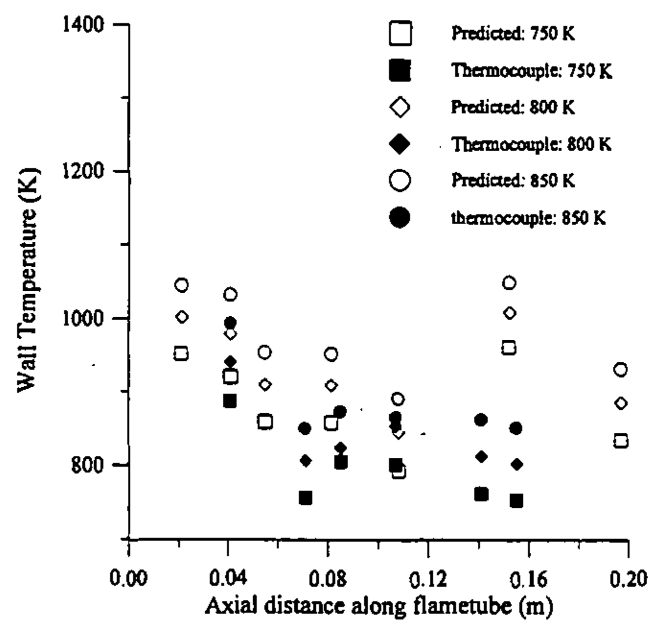

Figure 16; Influence of temperature on wall temperature at an inlet pressure of 9 bar.

Downloaded from http://asmedigitalcollection.asme.org/GT/proceedings-pdf/GT1999/78590/V002T02A011/4218414/v002t02a011-99-gt-059.pdf by guest on 01 July 2022